Taylor & Francis
Taylor & Francis Group

RESEARCH PAPER

CAF-like state in primary skin fibroblasts with constitutional *BRCA1* epimutation sheds new light on tumor suppressor deficiency-related changes in healthy tissue

Anna Etzold[a], Danuta Galetzka[a], Eva Weis[a], Oliver Bartsch[a], Thomas Haaf[b], Claudia Spix[c], Timo Itzel[c], Susann Schweiger[a], Dennis Strand[d], Susanne Strand[d,*], and Ulrich Zechner[a,*]

[a]Institute of Human Genetics, University Medical Center of the Johannes Gutenberg University Mainz, Mainz, Germany; [b]Institute of Human Genetics, Julius Maximilians University, Würzburg, Germany; [c]Institute of Medical Biometry, Epidemiology and Informatics, University Medical Center of the Johannes Gutenberg University Mainz, Mainz, Germany; [d]First Department of Internal Medicine, University Medical Center of the Johannes Gutenberg University Mainz, Mainz, Germany

ABSTRACT

Constitutive epimutations of tumor suppressor genes are increasingly considered as cancer predisposing factors equally to sequence mutations. In light of the emerging role of the microenvironment for cancer predisposition, initiation, and progression, we aimed to characterize the consequences of a *BRCA1* epimutation in cells of mesenchymal origin. We performed a comprehensive molecular and cellular comparison of primary dermal fibroblasts taken from a monozygous twin pair discordant for recurrent cancers and *BRCA1* epimutation, whose exceptional clinical case we previously reported in this journal. Comparative transcriptome analysis identified differential expression of extracellular matrix-related genes and pro-tumorigenic growth factors, such as collagens and CXC chemokines. Moreover, genes known to be key markers of so called cancer-associated fibroblasts (CAFs), such as *ACTA2, FAP, PDPN*, and *TNC*, were upregulated in fibroblasts of the affected twin (*BRCA1*^{mosMe}) in comparison to those of the healthy twin (*BRCA1*^{wt}). Further analyses detected CAF-typical cellular features, including an elevated growth rate, enhanced migration, altered actin architecture and increased production of ketone bodies in *BRCA1*^{mosMe} fibroblasts compared to *BRCA1*^{wt} fibroblasts. In addition, conditioned medium of *BRCA1*^{mosMe} fibroblasts was more potent than conditioned medium of *BRCA1*^{wt} fibroblasts to promote cell proliferation in an epithelial and a cancer cell line. Our data demonstrate, that a CAF-like state is not an exclusive feature of tumor-associated tissue but also exists in healthy tissue with tumor suppressor deficiency. The naturally occurring phenomenon of twin fibroblasts differing in their *BRCA1* methylation status revealed to be a unique powerful tool for exploring tumor suppressor deficiency-related changes in healthy tissue, reinforcing their significance for cancer predisposition.

Introduction

Cancer is generally referred to as a genetic disease. However, epigenetic aberrations are also hallmarks of cancer formation, which lead to gene expression changes without affecting the DNA sequence.[1-3] Cancer evolution is associated with both global DNA hypomethylation, leading to genomic instability, and a more specific hypermethylation of promoters of tumor suppressor genes, inducing their silencing.[1,2,4,5] The latter not only arises in neoplastic cells but can also occur as soma-wide constitutional epimutations, increasingly considered as a first hit according to Knudson's hypothesis. As somatic mosaicism is a common facet of epimutations, it suggests that the originating events occur after fertilization during early embryo development. However, there is also increasing evidence for the existence of germline epimutations, such as epigenetic aberrations in *MLH1* and *MSH2* in cases of familial colorectal cancer.[6-8]

We previously described a 29-year-old patient with recurrent cancers that harbors a mosaic epimutation of *BRCA1* in contrast to her healthy monozygous twin sister.[9] The constitutive *BRCA1* epimutation in one quarter of the patient's cells manifested as an elevated *BRCA1* promoter methylation level in DNA from saliva and dermal fibroblasts and was identified as the most likely cause for the difference in cancer proneness.

BRCA1 is a genomic caretaker gene that when mutated is responsible for a strong cancer predisposition, in particular for the hereditary forms of early-onset breast and ovarian cancers. Hypermethylation of the *BRCA1* promoter was found to be present in a subset of blood cells of mutation-negative breast and ovarian cancer patients, suggesting that epigenetic disruption of *BRCA1* may be an alternative, but equivalent, mechanism to genetic alterations for cancer predisposition.[10] Furthermore, in absence of sequence mutations, promoter hypermethylation of *BRCA1* and its complete silencing correlate with BRCAness of breast tumors in terms of histopathological characteristics and also therapy response.[11-13] The pathomechanism by which *BRCA1* sequence or epimutations

promote cancer formation is still not fully understood. Deficiency in DNA repair capability, which is generally considered as a causal factor for cancer proneness, could only be shown *in vitro* for cancer cells or cell lines but never for human primary cells harboring *BRCA1* mutations.[14] In light of some recent findings that cancer is not an isolated entity but stands in symbiosis with tumor microenvironment, studying the role of *BRCA1* in stromal cells of mesenchymal origin, such as fibroblasts, is also important, but has been neglected in the past. However, first *in vitro* studies have already shown that *BRCA1* deficiency leads to altered features of stromal cells potentially modulating stromal-epithelial interactions in a pro-tumorigenic manner.[15]

We have analyzed molecular and cellular features of primary dermal fibroblasts taken from our patient with the mosaic *BRCA1* epimutation (*BRCA1*^mosMe) compared to control fibroblasts of the healthy twin sister (*BRCA1*^wt), giving us the unique chance to explore the consequences of *BRCA1* deficiency in an genetically nearly identical system of somatic mesenchymal cells. We determined a differential gene expression profile highly consistent with that described for cancer-associated fibroblasts (CAFs) as well as CAF-typical cellular features including a significant increase in cell proliferation, migration, ketone production, and altered actin architecture. In addition, conditioned medium of the *BRCA1*^mosMe fibroblasts similar to that of CAFs enhanced growth of tumor cells *in vitro*. Together, our data strengthen the hypothesis that constitutive *BRCA1* epimutation modulates the phenotypic and functional characteristics of primary fibroblasts toward a state that provides a favorable environment for cancer formation.

Results

BRCA1 mRNA and protein expression is reduced in BRCA1^mosMe fibroblasts in comparison to BRCA1^wt fibroblasts

We analyzed *BRCA1* expression at the mRNA and protein level for an initial characterization of the epigenetically mediated *BRCA1* haploinsufficiency. Using quantitative reverse transcription PCR (RT-qPCR), *BRCA1*^mosMe fibroblasts exhibited a *BRCA1* mRNA expression that is 29% lower and significantly different from that of *BRCA1*^wt fibroblasts (Fig. 1A, $P = 0.017$). Although immunodetection of BRCA1 in primary non-neoplastic cells is known to be challenging,[16] we succeeded in detecting 220 kDa bands representing BRCA1 protein in the Western blot analysis and determined a definite difference in band intensities between the two samples (Fig. 1B). Band quantification and normalization to ACTIN control showed that the BRCA1 protein level in *BRCA1*^mosMe fibroblasts is 32% lower compared to that in *BRCA1*^wt fibroblasts (Fig. 1B).

Comparative transcriptome analysis shows stable expression differences between BRCA1^mosMe fibroblasts and BRCA1^wt control fibroblasts

To investigate molecular changes that result from the *BRCA1* epimutation in our patient's fibroblasts we first conducted a comparative genome wide expression array analysis on four separately cultured samples of *BRCA1*^mosMe fibroblasts and *BRCA1*^wt fibroblasts using the Affymetrix U219 array. In the subsequently performed analysis of variance (ANOVA) for the identification of differentially expressed genes (DEGs), rather loose filtering criteria were used to include all relevant genes and to compensate for the fact that our sample of interest is a mixture of affected and unaffected cells. We set the fold change threshold for differentially expressed probe sets to 1.5 and the *P*-value to 0.05. The ANOVA analysis revealed 133 probe sets accounting for 91 genes that were significantly upregulated and 243 probe sets, representing 194 genes, that were significantly downregulated in *BRCA1*^mosMe fibroblasts compared to *BRCA1*^wt fibroblasts (Tables S1 and S2). Hierarchical clustering of the prefiltered probe set list resulted in two clusters of four samples that belonged to the patient and to the healthy twin sister, respectively (Fig. 1C), indicating that the expression profile is stable through fibroblast culture and specific to the fibroblast donor.

Validation of the expression differences of 10 selected genes between *BRCA1*^mosMe fibroblasts and *BRCA1*^wt fibroblasts by qRT-PCR showed consistency between microarray and qRT-PCR results in terms of a generally consistent trend and extent of differential expression between the two samples (Fig. S1).

BRCA1^mosMe fibroblast overexpress extracellular matrix (ECM)-associated genes and pro-tumorigenic cytokines

Next we investigated the functional importance of the expression signature of *BRCA1*^mosMe fibroblasts by gene ontology enrichment analysis with the "Database for Annotation, Visualization and Integrated Discovery" (DAVID) tool in more detail. To avoid overlapping effects, we decided to analyze the upregulated and the downregulated parts of the DEG list separately. For the upregulated genes we found that terms associated to the extracellular space and the extracellular matrix were highly enriched in the cellular component analysis (Table 1). The analysis of biological processes fittingly showed a significant enrichment of processes that take place in the surrounding of cells, such as cellular and biological adhesion, extracellular structure, and matrix organization. These term enrichments can be traced back to a large extent to genes encoding extracellular structural proteins such as collagens (COL1A1, COL5A1 COL11A1, COL8A1, and COL12A1) and filaggrin (FLG) that are highly overrepresented on the upregulated list (Fig. 1C and Table S1). Furthermore, a variety of genes encoding proteins involved in ECM remodeling, such as *MGP, POSTN*, or *TNC*, represent a huge part of the specific signature of *BRCA1*^mosMe fibroblasts. Moreover, there is also a significant upregulation of genes encoding some cytokines and growth factors, including, for example, *CXCL12, CXCL6*, and *IL6*. These genes play important roles in processes like cell adhesion, cell motion, and cell differentiation, which were also revealed by gene ontology (GO) analysis.

The expression profile of BRCA1^mosMe fibroblasts shows a downregulation of HOX genes and suggests an inhibition of BRCA1-related DNA repair

A significant portion of downregulated genes in the *BRCA1*^mosMe fibroblast expression profile belongs to the HOX gene family and, consistently, the GO biological processes analysis showed a strong enrichment of associated
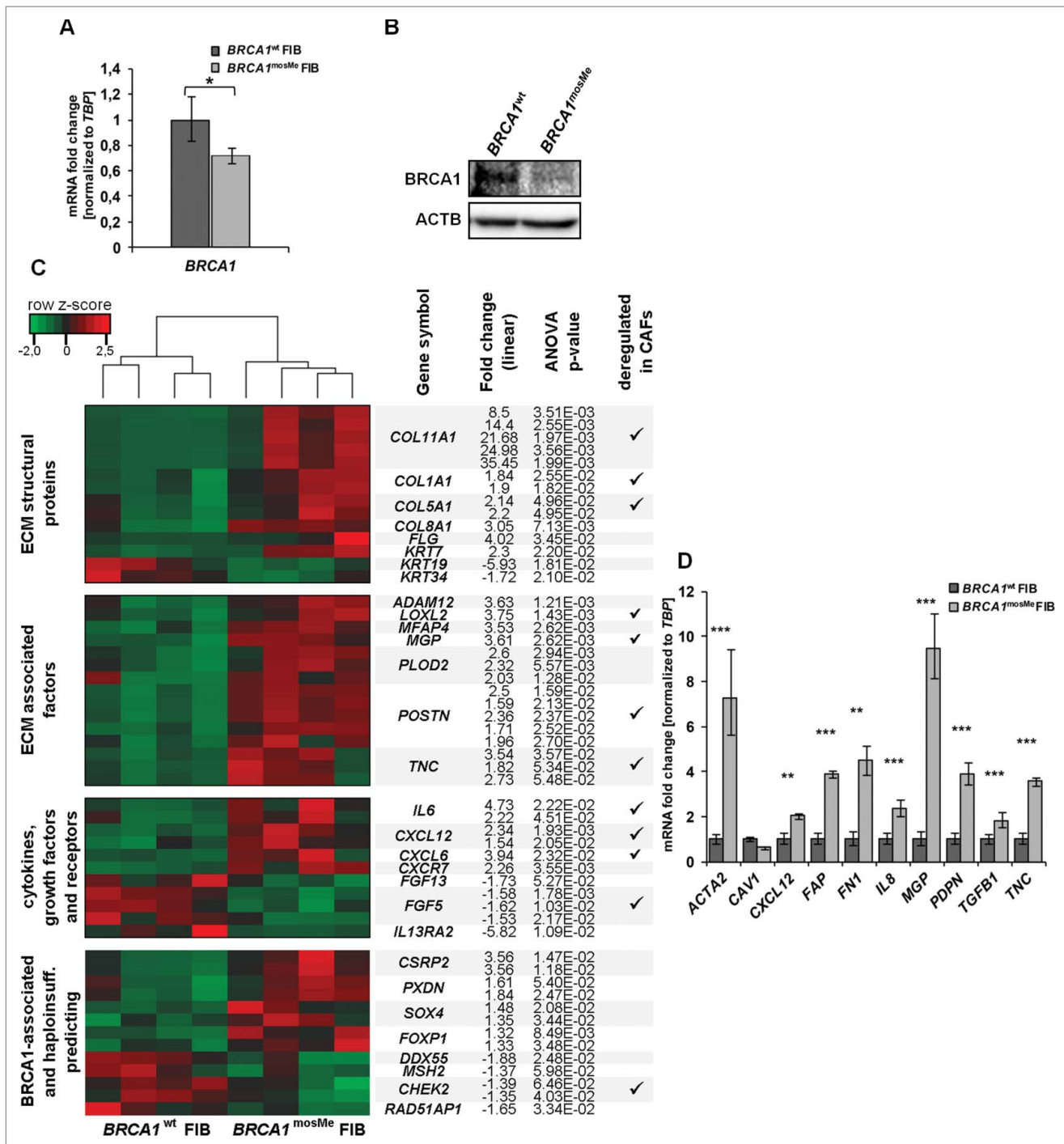
Figure 1. (A) RT-qPCR analysis of *BRCA1* mRNA expression, normalized to TBP and standardized to expression of *BRCA1*wt fibroblasts (FIB) (n = 3,*P < 0.05). (B) Western blot analysis of BRCA1 protein in 150μg total cell extracts of *BRCA1*mosMe fibroblasts and *BRCA1*wt fibroblasts using anti-BRCA1 antibody. Immunoblotting for ACTIN serves as loading control. (C) Heatmap showing CAF-related selection of differentially expressed transcripts between *BRCA1*wt fibroblasts and *BRCA1*mosMe fibroblasts. Hierarchical clustering of DEGs was performed using the complete linkage method. (D) RT-qPCR analysis of CAF keyplayers (n = 3, * P < 0.05, **P < 0.0005, ***P < 0.00005).

terms. HOX gene expression profiles in dermal fibroblasts display a positional memory and are known to be variable depending on minimal differences in the localization from which the biopsy was taken.[17] To exclude overestimation of such effects and avoid possible masking of other important results by the very strong expression changes of HOX genes, we have repeated the GO analysis with the downregulated gene list after exclusion of HOX genes (Table 2). There was still an enrichment of terms associated with the

ECM. However, in contrast to the GO analysis of upregulated genes, the ECM term enrichment could be attributed to the downregulation of secreted growth factors such as *FGF13* and *FGF6*, rather than structural proteins or ECM-modulating enzymes. Interestingly, some of the accumulated biological processes and molecular function analysis terms were linked to DNA damage and repair, such as nucleotide kinase activity or double strand break repair. Many of these enriched terms included *BRCA1*, which we

Table 1. DAVID gene ontology and pathway analysis of upregulated genes[1].

GO terms Cellular Component				GO terms Biological Process			
GO:	Term	No.	P-value	GO:	Term	No.	P-value
0044421	extracellular region part	27	1.70E-11	0007155	cell adhesion	18	1.63E-07
0005578	proteinaceous extracellular matrix	17	4.57E-11	0022610	biological adhesion	18	1.65E-07
0031012	extracellular matrix	17	1.40E-10	0043062	extracellular structure organization	9	2.87E-06
0044420	extracellular matrix part	9	4.35E-07	0030198	extracellular matrix organization	7	2.17E-05
0005581	collagen	5	5.25E-05	0035295	tube development	9	2.58E-05
0005604	basement membrane	5	1.18E-03	0051094	positive regulation of developmental	9	1.34E-04
0005583	fibrillar collagen	3	2.22E-03	0007517	muscle organ development	8	1.51E-04
0005615	extracellular space	12	2.29E-03	0006928	cell motion	11	2.48E-04
0005795	Golgi stack	4	2.55E-03	0045597	positive regulation of cell differentiation	8	2.50E-04
0008282	ATP-sensitive potassium channel complex	2	1.77E-02	0001501	skeletal system development	9	9.51E-01

GO terms Molecular Function				KEGG pathways			
GO:	Term	No.	P-value	hsa code	Pathway	No.	P-value
0005201	extracellular matrix structural constituent	6	7.93E-05	004512	ECM-receptor interaction	5	1.37E-03
0019838	growth factor binding	6	2.04E-04	004510	Focal adhesion	6	5.84E-03
0005509	calcium ion binding	15	2.05E-04	005410	Hypertrophic cardiomyopathy (HCM)	4	1.32E-02
0005198	structural molecule activity	11	1.43E-03	004350	TGF-beta signaling pathway	4	1.41E-02
0046872	metal ion binding	33	4.75E-03	004060	Cytokine-cytokine receptor interaction	5	6.58E-02
0043169	cation binding	33	5.56E-03				
0043167	ion binding	33	7.10E-03				
0005539	glycosaminoglycan binding	4	3.56E-02				
0030247	polysaccharide binding	4	4.52E-02				
0000187	pattern binding	4	4.52E-02				

[1]genes that are more than 1.5-fold upregulated with a P-value smaller than 0.05

have shown to be downregulated by its epimutation in *BRCA1*^mosMe fibroblasts (Fig. 1A and 1B). Consistent with this, genes encoding binding partners of BRCA1, such as *MLH2, CHEK2*, and *RAD51AP1*, were also downregulated in the *BRCA1*^mosMe fibroblasts (Fig. 1C) and responsible for the enrichment of repair-associated terms in the GO analysis.

BRCA1^mosMe *fibroblasts reflect BRCA1 haploinsufficiency with an expression signature highly similar to that of CAFs*

To test if the fibroblasts contain expression changes in addition to those of the DNA-repair-associated genes that can be traced back to *BRCA1* haploinsufficiency, we compared our obtained signature to published data that had been produced on

Table 2. DAVID gene ontology and pathway analysis of downregulated genes[1].

GO terms Biological Process (incl. *HOX* genes)				GO terms Biological Process (excl. *HOX* genes)			
GO:	Term	No.	P-value	GO:	Term	No.	P-value
0009952	anterior/posterior pattern formation	9	8.33E-05	0009153	purine deoxyribonucleotide biosynthesis	2	1.90E-02
0003002	regionalization	9	8.43E-04	0010033	response to organic substance	14	2.01E-02
0048706	embryonic skeletal system development	6	1.06E-03	0006302	double-strand break repair	4	2.13E-02
0007389	pattern specification process	10	1.50E-03	0009719	response to endogenous stimulus	9	4.00E-02
0048568	embryonic organ development	8	1.76E-03	0009265	2'-deoxyribonucleotide biosynthesis	2	4.68E-02
0043009	chordate embryonic development	11	1.87E-03	0006072	glycerol-3-phosphate metabolism	2	5.59E-02
0009792	embryonic development ending in birth	11	2.00E-03	0016053	organic acid biosynthesis	5	6.09E-02
0048704	embryonic skeletal system morphogenesis	5	2.56E-03	0046394	carboxylic acid biosynthesis	5	6.09E-02
0001501	skeletal system development	10	4.92E-03	0018065	protein-cofactor linkage	2	7.38E-02
0048705	skeletal system morphogenesis	6	5.42E-03	0009263	deoxyribonucleotide biosynthesis	2	7.38E-02

GO terms Cellular Component (excl. *HOX* genes)				GO terms Molecular Function (excl. *HOX* genes)			
GO:	Term	No.	P-value	GO:	Term	No.	P-value
0043005	neuron projection	8	2.82E-02	0042802	identical protein binding	13	193E-02
0044421	extracellular region part	14	6.85E-02	0003747	translation release factor activity	2	5.60E-02
0042995	cell projection	11	7.71E-02	0008079	translation termination factor activity	2	5.60E-02
0005739	mitochondrion	15	8.28E-02	0019205	nucleobase, nucleoside, nucleotide kinase act.	3	6.34E-02
0031233	intrinsic to external side of plasma membrane	2	8.28E-02	0003697	single-stranded DNA binding	3	9.69E-02
0005576	extracellular region	24	8.89E-02	0004896	cytokine receptor activity	3	9.69E-02

KEGG pathways (excl. *HOX* genes)			
hsa code	Pathway	No.	p-value
00270	Cysteine and methionine metabolism	3	5.17E-02

[1]genes that are more than 1.5-fold downregulated with a P-value smaller than 0.05

lymphocytes to identify *BRCA1* mutation carriers based on their expression profiles.[18] When using our original filtering criteria, we found an overlap of about 10%. Considering the fact that our sample represents a *BRCA1* haploinsufficiency present in a ˜25% mosaic, we also included genes whose expression differed significantly but only minimally to an extent of 25% and thereby found an overlap of 25% between our *BRCA1*^mosMe fibroblast profile and the signature predicting *BRCA1* mutation carrier status. Shared genes were, for example, *PXDN, CSRP2, ENPP2,* and *FOXP1* (Fig. 1C). However, the by far larger portion of deregulated genes in *BRCA1*^mosMe fibroblasts and, in particular, the overexpression of ECM-associated genes, cytokines, and growth factors could not be directly explained and connected to *BRCA1* disruption. For this reason, we searched in the literature if these expression changes had already been described for primary fibroblasts in any conditions. We found a massive concordance of our *BRCA1*^mosMe fibroblast profile with the expression signature of CAFs. This overlap mainly involved the genes that constitute the core signature of CAFs, being equally deregulated in CAFs isolated from a variety of different tumor types, in contrast to normal fibroblasts from the same tissue.

CAF keyplayer genes are deregulated in BRCA1^mosMe fibroblasts

To further verify the hypothesis that our *BRCA1*^mosMe fibroblasts share transcriptomic characteristics with CAFs, we specifically re-analyzed the expression of known CAF key genes with qRT-PCR. All analyzed genes showed the expected expression differences, based on the assumption that *BRCA1*^mosMe fibroblasts in contrast to *BRCA1*^wt fibroblasts have a CAF-like transcription profile (Fig. 1D). The fold changes of *ACTA2* and *FAP*, the most established CAF markers, were as high as 7.29 and 3.86, respectively. We also observed a strong, even though not significant, decrease (40%) of *CAV1* mRNA, which is a common feature of many types of CAFs. In addition, there were significant expression differences ranging from 1.8 to 9.5 in cytokines and ECM-related genes known to determinably trigger CAF-specific phenotypes and functions, such as *CXCL12, FN1, IL8, MGP, PDPN, TGFB1,* and *TNC.* Taken together, these results let us assume that the *BRCA1*^mosMe fibroblasts show transcriptional characteristics that demarcate them from the *BRCA1*^wt fibroblasts, in the same way CAFs differ from normal fibroblasts.

BRCA1^mosMe fibroblasts show accelerated proliferation and migration

Next, we investigated if *BRCA1*^mosMe fibroblasts also exhibit functional features of CAFs. We analyzed the growth rates of *BRCA1*^mosMe fibroblasts compared to *BRCA1*^wt fibroblasts, as an increased proliferative index is a common feature of CAFs. We established growth curves over 10 days for different culture passages testing every day for the amount of living cells by a luminescence assay. The increased growth rates of *BRCA1*^mosMe fibroblasts already manifested itself significantly at day 3 for passage 6 cells and even already at day 2 for passage 11 cells, and became more prominent in the course of the experiment (Fig. 2A). At day 10, *BRCA1*^mosMe fibroblasts demonstrated an increase of normalized Relative Light Unit (RLU) signals of 157 and 185 percentage points, respectively, compared to *BRCA1*^wt fibroblasts. Consistently, immunostaining against Ki-67 showed a 3-fold higher amount ($P < 0.05$) of Ki-67-positive cells in the *BRCA1*^mosMe fibroblast culture than in the control culture (Fig. 2B). Moreover, there was a small but significant increase in migratory capability of *BRCA1*^mosMe fibroblasts as determined by means of IBIDI chambers (Fig. 2C).

BRCA1^mosMe fibroblasts show changes in collagen abundance and actin architecture

As CAFs usually also strongly produce collagen, we immunostained *BRCA1*^mosMe fibroblasts for type I collagen to analyze this feature not only on the RNA but also on the protein level. All *BRCA1*^mosMe fibroblasts were positive for cell-associated collagen I in contrast to *BRCA1*^wt fibroblasts that displayed almost no collagen I staining (Fig. 3B).

Next, we visualized the cytoskeletal organization of *BRCA1*^mosMe fibroblasts using phalloidin staining. As predicted, *BRCA1*^mosMe fibroblasts showed a more organized actin skeleton characterized by a large number of thick and parallel F-actin-based stress fibers extending across the cell (Fig. 3A). In contrast, the staining in *BRCA1*^wt fibroblasts was weaker, and the actin skeleton looked more relaxed with the strongest staining along the membranes. Paxillin staining was much weaker in *BRCA1*^mosMe fibroblasts than in *BRCA1*^wt fibroblasts. However, in *BRCA1*^mosMe fibroblasts paxillin tended to show some punctual staining at the ends of stress fibers in contrast to *BRCA1*^wt fibroblasts, where the staining was completely diffuse and disorganized in particular around the nucleus. This observation can indicate that focal adhesion signaling is more active in *BRCA1*^mosMe fibroblasts than in the control fibroblasts.

Increased ketone body generation in BRCA1^mosMe fibroblasts

Metabolic reprogramming is a hallmark of CAFs, and fueling cancer cells with energy-rich metabolites is one way by which CAFs promote proliferation of surrounding cancer cells. To test if *BRCA1*^mosMe fibroblasts also show hallmarks for such a mitochondrial dysfunction, we compared the concentration of ketone bodies as energy-rich molecules between conditioned medium of *BRCA1*^mosMe fibroblasts and that of *BRCA1*^wt fibroblasts. We found the concentration of β-hydroxybutyrate to be reproducibly and significantly increased by more than two-fold in *BRCA1*^mosMe fibroblasts in comparison to *BRCA1*^wt fibroblasts (Fig. 3C).

Conditioned medium of BRCA1^mosMe fibroblasts enhances proliferation of cancer cells and non-neoplastic epithelial cells

Next, we investigated whether the potentially pro-tumorigenic features that we found in *BRCA1*^mosMe fibroblast actually have a similar influence on tumorous or non-tumorous epithelial cells as CAFs. We performed proliferation assays with the tumorous human lung adenocarcinoma epithelial
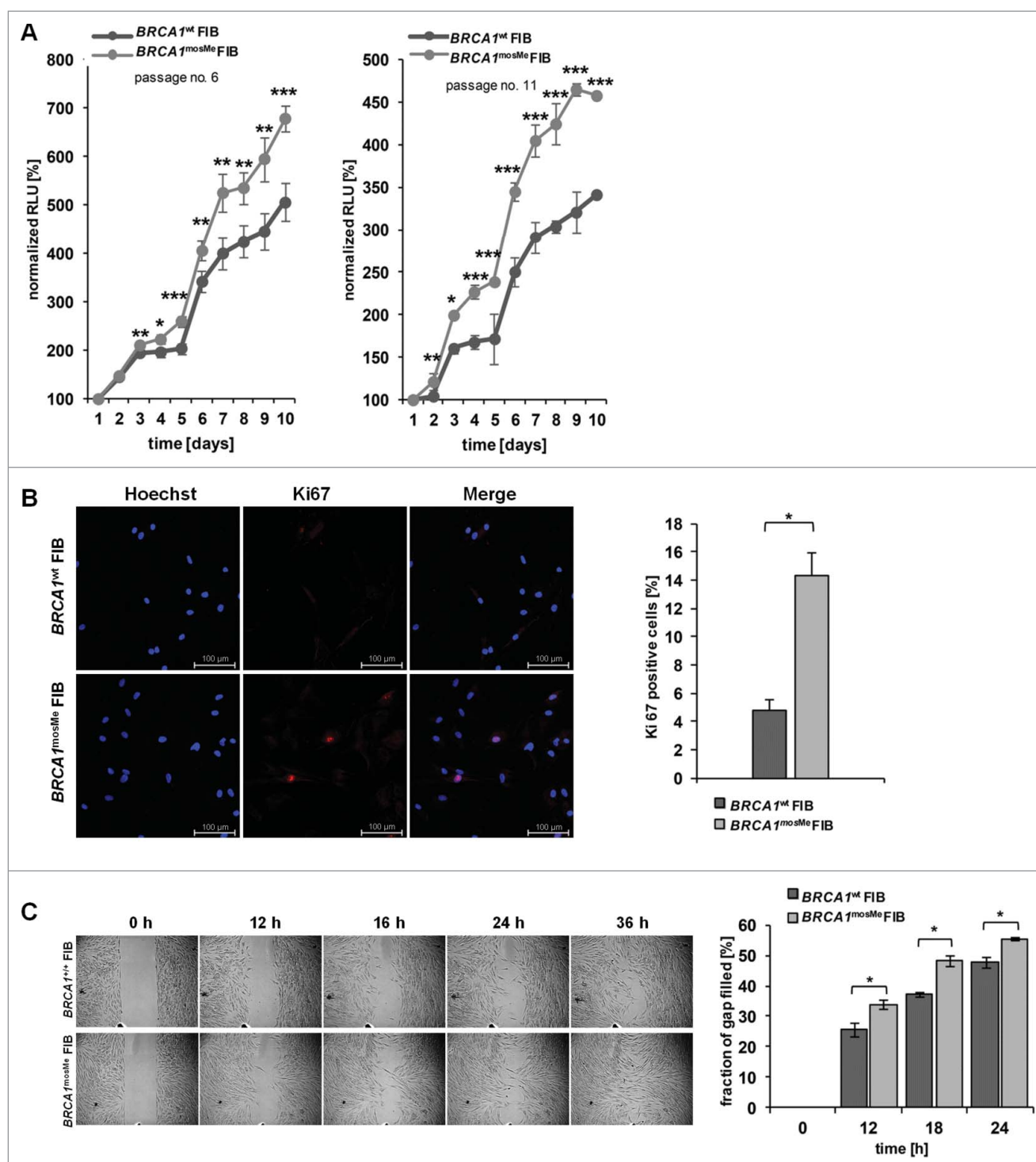
Figure 2. (A) Growth curves of *BRCA1*^{wt} and *BRCA1*^{mosMe} fibroblasts (FIB) as measured by Cell titer glo assay (n = 6, *P < 0.005, **P < 0.0005, ***P < 0.0005); RLU=Relative Light Units (B) Representative microphotographs of Ki-67 immunostaining of *BRCA1*^{wt} and *BRCA1*^{mosMe} fibroblasts and calculation of Ki-67 index (n = 3, *P < 0.05). (C) Migration assay of *BRCA1*^{wt} and *BRCA1*^{mosMe} fibroblasts and quantification (n=3, *P < 0.05).

cell line A549 and non-tumorous human mammary epithelial cell line (HLME) cells in the presence of conditioned medium of the fibroblast cultures. Growth of A549 cells fed with conditioned medium of *BRCA1*^{mosMe} fibroblasts started to differ from that of A549 cells cultured in conditioned medium of the control fibroblasts after four days of culture with a significant difference occurring only after five days of culture (Fig. 3D). The proliferation-enhancing effect of conditioned medium of *BRCA1*^{mosMe} fibroblasts on HLME cells was much stronger and already apparent on the second day of culture with a significant difference present throughout the whole experiment. These results suggest that *BRCA1*^{mosMe} fibroblasts not only show phenotypic features of CAFs but also harbor the ability to promote cell growth of cancer and epithelial cells.
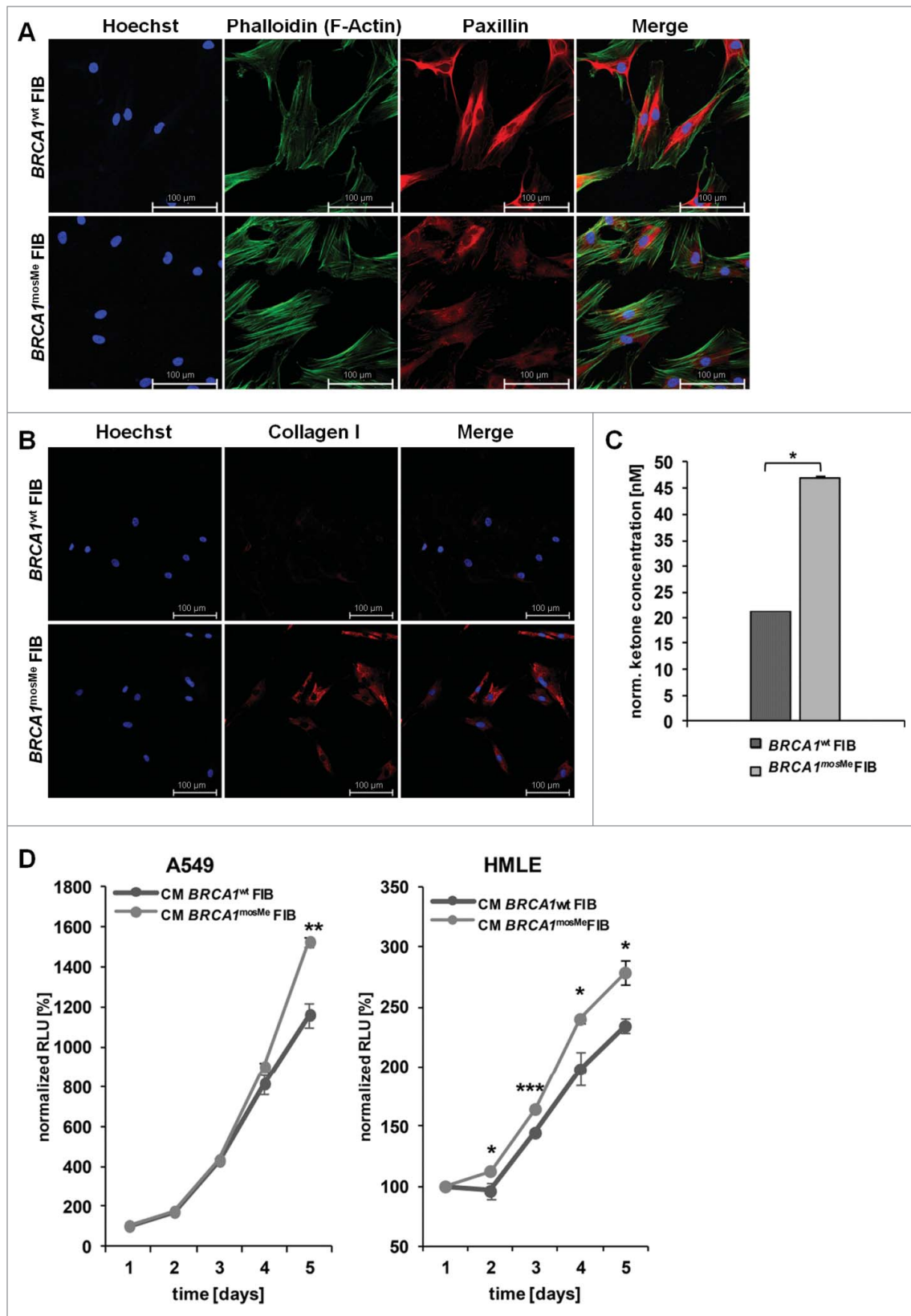
Figure 3. (A) Phalloidin staining of *BRCA1*[wt] and *BRCA1*[mosMe] fibroblasts (FIB). (B) Collagen I immunostaining of *BRCA1*[wt] and *BRCA1*[mosMe] fibroblasts. (C) Ketone concentrations of cell culture medium of *BRCA1*[wt] and *BRCA1*[mosMe] fibroblasts as determined by B-hydroxybutyrate assay ($n = 6$, $^{*}P < 0.05$). Values were normalized to protein mass per well. (D) Growth curves of a cancer cell line and a non-cancerous epithelial cell line cultured in conditioned medium of *BRCA1*[wt] and *BRCA1*[mosMe] fibroblasts as determined by Cell titer glo assay. ($n=5$, $^{*}P < 0.005$, $^{**}P < 0.0005$, $^{***}P < 0.0005$).

Discussion

CAFs are the major part of the tumor stroma and play a pivotal role in carcinogenesis and tumor progression.[19] A huge variety of cell types such as epithelial cells, mesenchymal stem cells, resident fibroblasts or endothelial cells have been reported to be able to transdifferentiate into CAFs through epithelial–mesenchymal transition (EMT), mesothelial-to-mesenchymal transition (MMT), or endothelial-mesenchymal transition (EndMT).[20-24] All these models for CAF development assume exogenous stimuli that initiate transformation and, in most cases, are thought to be sent from adjacent cancer cells in form of growth factors, such as TGF-ß and CXCL12.[23]

There is experimental evidence that the CAF phenotype can also be initiated by intrinsic factors. In particular depletion of tumor suppressor genes was reported to convert normal fibroblasts to CAFs.[15,25,26] As a result the question arises, if constitutional disruption of tumor suppressors may also provoke a CAF-like state *in vivo* in healthy tissue of persons epigenetically predisposed to hereditary cancers.

In the current study, we systematically compared for the first time primary fibroblasts affected by epigenetically mediated haploinsufficiency of the tumor suppressor *BRCA1* to CAFs and found remarkable similarities on the molecular, cellular, and functional level. We showed that key transcriptional features of CAFs, such as increased expression of pro-tumorigenic genes and ECM-associated genes, can also be detected in our *BRCA1*^mosMe fibroblasts, although taken from healthy non-neoplastic tissue. Ingenuity identified *TWIST1, TGF-ß, CXCL12, IL6, TNF*, and ethanol as possible upstream regulators, i.e., effectors of these expression changes (Fig. S2). As all these factors are important regulators or inducers of the CAF phenotype,[27-30] it stands to reason that the transcriptional program of *BRCA1*^mosMe fibroblasts actually resembles that of CAFs. To our knowledge, a CAF-like expression signature was only detected once before in healthy skin of individuals predisposed to basal cell carcinoma by mutations in the tumor suppressor gene *PTCH1*.[31] As *BRCA1* was reported to regulate *PTCH1* and other genes in Hedgehog pathways,[32] a convergent mechanism in induction of the CAF phenotype may be suspected.

We demonstrated that *BRCA1*^mosMe fibroblasts display an accelerated proliferation and migration compared to control fibroblasts. This finding is comparable to previous studies that described skin fibroblasts from individuals with hereditary breast cancer and from their relatives to have abnormal cellular phenotypes, including altered migratory behavior and proliferation.[33,34] From today's perspective, the similarities between these anomalies and those of CAFs are eye-catching, as a high proliferative index and increased motility are common features of CAFs from all different sources. Moreover, *in vitro* disruption of *BRCA1* by knockdown in fibroblasts, as well as epithelial cells and cancer cell lines, was also shown to accelerate cell proliferation.[15,35,36]

Cytoskeletal changes observed in *BRCA1*^mosMe fibroblasts, like bundling of actin stress fibers and also upregulation of α-smooth muscle actin (α-SMA) on mRNA level, are a known key feature of activated fibroblasts, such as myofibroblasts and also CAFs. The formation of stress fibers is required for matrix organization and remodeling,[37] which is a major function of CAFs in building a favorable environment for cancer growth and metastasis. In dermal fibroblasts of individuals predisposed to retinoblastoma, polyposis coli, and basal cell carcinoma, an increased actin content and an accelerated actin reorganization were found,[38] indicating that this kind of change seems to be common to cancer-predisposed fibroblasts independent of the tumor suppressor gene causally affected.

CAFs are known to fuel growth of neighboring cancer cells by supplying energy-rich metabolites such as lactate and ketones, which is named "reverse Warburg effect" or "two-compartment tumor metabolism".[39,40] In several studies, CAFs from different sources were shown to produce more ketone bodies than paired normal fibroblasts. Ketone elevation was also detected for *BRCA1*^mosMe fibroblasts in contrast to twin control fibroblasts in the current study, although cells were neither taken from malignant tissue nor co-cultured with cancer cells *in vitro*. It was previously hypothesized that the first step of metabolic reprogramming of CAFs is production of oxidative stress by cancer cells that subsequently leads to DNA damage in CAFs, which in turn triggers autophagy and mitochondrial degradation, causing shifts of the metabolism to aerobic glycolysis.[40-42] This process is crucially regulated by elevation of HIF-1α, which, in turn, is depending on BRCA1.[43,44] As BRCA1 seems to be an emerging regulator of mitochondrial integrity, we hypothesize that its disruption in primary fibroblasts of persons with germline or somatic alterations also may induce CAF-like metabolic changes in the absence of cancer cells. This is supported by experimental data from a stable knockdown of *BRCA1* in immortalized fibroblasts that results in upregulation of *HIF-1α*, autophagy, and ketone body production.[15] In addition, *BRCA1*-knockdown fibroblasts were shown to enhance cancer cell line proliferation when co-injected into xenografts. This effect is known from CAFs taken from tumor tissue.

Moreover, it was demonstrated that conditioned medium of CAFs is enough to enhance cancer cell proliferation in *in vitro* experiments,[45,46] probably due to secretion of tumorigenic growth factors and energy-rich metabolites. In the current study, we observed a comparable effect when culturing A549 lung carcinoma cells and non-tumorous HMLE mammary epithelial cells in the presence of conditioned medium of *BRCA1*^mosMe fibroblasts. This strongly supports our hypothesis that *BRCA1* epimutation in our proband's fibroblasts induces phenotypic, molecular, and functional changes resembling features of CAFs. Considering the data of Salem et al.[15] that show comparable changes in a *shBRCA1* fibroblast cell line, it stands to reason that the observed phenotype in *BRCA1*^mosMe fibroblasts is causally linked to the downregulation of *BRCA1*. Nevertheless, the copy number variations of the genes *RSPO3* and *NREP (C5orf13)*, which we previously reported to be present in a 50% mosaic in the analyzed cells,[9] could also play a contributory role that was not specifically analyzed in this study. *RSPO3* acts as a proto-oncogene whose gain-of-expression promotes tumorigenic processes. In contrast, a reduction of *RSPO3*

expression, which is the consequence of the mosaic *RSPO3* deletion in our proband's cells,[9] was already linked to the opposite of our findings, namely a reduction in cell proliferation and migration, in *RSPO3* knockdown cancer cells.[47,48] The expression of *NREP* in *BRCA1*[mosMe] was unaffected by the deletion[9] and no connection of this gene to cancerogenesis is known to date. It is beyond the scope of our present study, but remains to be determined, whether the deletions of *RSPO3* and *NREP* co-exist with the *BRCA1* epimutation in the same cells of the *BRCA1*[mosMe] fibroblasts.

Based on our findings, we speculate that epigenetic *BRCA1* deficiency in predisposed persons may lead to a CAF-like state of stromal cells prior to cancer onset and perhaps even from birth on. This CAF-like state may promote tumorigenic transformation of neighboring epithelial cells by altered stromal-epithelial interactions and thereby explain the predisposition of the mutation carriers to carcinogenic conditions.

If this concept is proven to be generally applicable to mesenchymal cells also with *BRCA1* sequence mutations, it may open completely new perspectives on hereditary *BRCA1*-related carcinogenesis and provide impetus for the development of new preventive strategies. According to this idea, therapeutic approaches for cancer treatment targeting the tumor microenvironment are already in clinical trials, and can possibly be transferred to the prevention of tumor development in hereditary cancers by interfering either with the maintenance of the CAF-like state of fibroblasts or with the secretion of protumorigenic signals.[49] Another potential strategy for chemoprevention is to compensate for oxidative stress that leads to mitochondrial dysfunction and autophagy and shifting of the metabolism in *BRCA1* deficient cells.[15] Interestingly, antioxidant treatment just like genetic complementation of *BRCA1* in *BRCA1* null breast cancer cells reverts functional markers of oxidative stress, namely CAV1 loss and MCT4 induction in co-cultured fibroblasts.[50]

In conclusion, we have shown an example of transcriptional and functional CAF-like state existing in fibroblasts of healthy tissue, which was probably induced by epigenetically mediated *BRCA1* haploinsufficiency. Thus, we suggest building a favorable environment for cancer development and growth by CAF-like fibroblasts to be one of many mechanisms by which cancer proneness is mediated in individuals with *BRCA1* epimutation. This hypothesis brings many new potential targets for cancer prevention in genetically predisposed individuals into play.

Materials and methods

Case presentation

The biological material that was analyzed in this study was taken from a proven monozygous twin pair with discordance for recurrent cancers. First cancer occurred in the affected individual at an age of 4 years and was characterized as precursor B-cell lymphoblastic leukemia. Thyroid carcinoma was diagnosed at an age of 25 years. The affected twin was the only individual being suffering from cancer in the family pedigree including four generations. The clinical case has been previously described in more detail in Galetzka et al.[9]

Isolation and culture of primary fibroblasts

Genetic counseling was offered and informed written consent was obtained from both probands. This study was approved by the Ethics Committee of the Medical Association of Rhineland-Palatinate (No. 837.440.03[4102]). Skin biopsies were taken from the probands at an age of 29 years from the left upper arm, and fibroblasts cultures were established. Cells were cultured in their original primary state without immortalization or any other genetic manipulation. The fibroblasts were cultured in Dulbecco's modified eagles medium (Thermo Fisher Scientific, #11960) supplemented with 10% fetal calf serum (Thermo Fisher Scientific, #10270) and penicillin-streptomycin (Thermo Fisher Scientific, # 15070063). The cells were passaged and harvested at subconfluency.

Gene expression microarray analysis

The array experiment was performed by Affymetrix using the GeneAtlas[TM] Personal Microarray System (Affymetrix). RNA samples extracted from primary fibroblasts using TRIzol reagent (Thermo Fisher Scientific, #15596) were hybridized on a HG-U219 array strip (Affymetrix). Microarray data have been deposited at the Gene Expression Omnibus (GEO) database with the accession number GSE71078. Data normalization by Robust Multi-array Average (RMA) approach and analysis of differentially expressed probe sets by Tukey's Bi-weight average algorithm and Analysis of Variance (ANOVA) were done with Affymetrix Expression Console Software and Affymetrix Transcriptome Analysis Console respectively. Functional enrichment, network analysis and upstream regulator analysis were performed using Database of Annotation, Visualization and Integrated Discovery (DAVID)[51] and Ingenuity Pathways Analysis tool (Qiagen).

Quantitative real time PCR

RNA was extracted using TRIzol® reagent (Thermo Fisher Scientific) and RNA quality and purity were checked photometrically. Reverse transcription reaction was performed by means of SuperScript® III RT kit (Thermo Fisher Scientific) using a combination of random and oligo (dT) primers. Primers for real time PCR were designed with Primer3 version 4.0.0 as detailed in Table S3 and commercially available primers for *TBP* served as endogenous control (Qiagen QuantiTect #QT00000721).[52] Data acquisition was performed with the StepOnePlus Real-Time PCR System with following PCR cycling conditions: 40 cycles of 30 sec at 95°C, 30 sec at 60°C and 40 sec at 72°C. To avoid and check for genomic contamination, primers were designed exon spanning, water and minus-reverse-transcriptase controls were included and melting curve analysis was done. Comparative $2^{-\Delta\Delta Ct}$ method was used for relative quantification of gene expression with error bars indicating $\pm RQ_{min/max} = 2^{[\Delta\Delta Ct \pm T^*SD(\Delta Ct)]}$ as

T = confidence level and SD = standard deviation. Statistical analysis was performed using the student's t-test and *P*-values ≤ 0.05 were considered statistically significant.

Immunoblot analysis

Protein extraction was performed according to Bräutigam et al.[53] Different amounts of total protein were separated on a 6% acrylamide gel for BRCA1 blotting and on a 10% acrylamide gel for later ACTIN blotting. Western Blot analyses were performed with anti-BRCA1 (Merck Millipore, MS110, #MABC 199) and anti-ACTIN (Sigma Aldrich, #A2228) respectively, as primary antibodies, and HRP-coupled anti-rabbit and anti-mouse (Dianova, #111–036, 111–035), respectively, as secondary antibodies. Signal detection was achieved by ChemiDoc XRS digital imager (Biorad). The software Chemi-Doc Image Lab (Biorad) was used for densitometric analyses of BRCA1 bands and normalization to ACTIN band intensities.

Immunofluorescence microscopy

Equal amounts of *BRCA1*^{mosMe} and *BRCA1*^{wt} fibroblasts were seeded in chamber well slides and grown over night. Cells were fixed in 4% paraformaldehyde (PFA), blocked in 3% BSA in PBST and permeabilized in 0.2% saponin (Carl Roth, #6857). The slides were sequentially probed with primary and secondary antibodies or stained with Fluor-488-Phalloidin (Thermo Fisher Scientific, #A12379). Nuclei were stained with Hoechst 33342 (Thermo Fisher Scientific, #62249). The primary antibodies used were mouse anti-human paxillin (R&D Systems, #AF4259), rabbit anti-human Ki67 (Thermo Fisher Scientific, #RM-9106) and mouse anti-human collagen I (Abcam, #ab88147) the secondary antibodies used alexa-flour-488 mouse anti-rabbit, alexa-flour-488 goat anti-mouse and alexa-flour-546 goat anti rabbit (Thermo Fisher Scientific, #11059, #11001, #11035). The slides were imaged by Zeiss confocal laser scan microscope CLSM 710-NLO.

Proliferation assays of fibroblasts and conditioned medium proliferation assays of HMLE and A549 cells

The proliferation assays were conducted with the CellTiter-Glo Luminescent Cell Viability Assay (Promega, #G7570) according to the manufacturer's protocol. In brief, 2,000 fibroblasts were seeded per well in a 96 well plate. On the next day and then every 24 hours cell viability was measured and values were normalized to the first measurement.

For conditioned medium proliferation assays 2000 HMLE cells or 500 A549 cells were seeded in a 96 well plate, respectively. On the next day the medium was changed to either conditioned medium of *BRCA1*^{mosMe} fibroblasts or *BRCA1*^{wt} fibroblasts. The conditioned medium had been prepared by cultivation of 500,000 exponentially growing fibroblasts in 3 ml of DMEM for 72 hours. Cell debris was separated by centrifugation at 4000 rpm for 10 minutes, and the conditioned medium was stored at −80°C.

Fibroblast migration assays

Fibroblasts (12,000) were seeded in 70 μl medium into each chamber of a culture insert (IBIDI, #80206). After 24 hours the silicone inserts were removed and the gap between the cell fields was photographed every 6 hours in the same optical field. The pictures were analyzed using the Scratch Assay Analyzer plugin from the extension package MiToBo in ImageJ.

Quantification of ketone bodies

Fibroblasts (100,000/per well) were plated in a 24-well plate in complete media. The next day the cells were washed twice with dPBS and the medium was changed to optiMEM (Thermo Fisher Scientific, #31985062) containing 2% FBS. After 48 hours of incubation the cell culture supernatant was collected and separated from cell debris by centrifugation. The concentration of ketone bodies was determined using the β-hydroxybutyrate assay (Sigma Aldrich, #MAK041).

Statistical analysis

If not indicated differently, the values are given as mean ± standard error of the mean (SEM). The Student t-test was performed for statistical analysis. *P*-values ≤ 0.05 were considered to be statistically significant.

Disclosure of potential conflicts of interest

No potential conflicts of interest were disclosed.

Acknowledgments

References

1. Ehrlich M. DNA methylation in cancer: too much, but also too little. Oncogene 2002; 21:5400-13; PMID:12154403; http://dx.doi.org/10.1038/sj.onc.1205651
2. Sharma S, Kelly TK, Jones PA. Epigenetics in cancer. Carcinogenesis 2010; 31:27-36; PMID:19752007; http://dx.doi.org/10.1093/carcin/bgp220
3. Jaenisch R, Bird A. Epigenetic regulation of gene expression: how the genome integrates intrinsic and environmental signals. Nat Genet 2003; 33:245-54; PMID:12610534; http://dx.doi.org/10.1038/ng1089
4. De Smet C, Loriot A. DNA hypomethylation in cancer: epigenetic scars of a neoplastic journey. Epigenetics 2010; 5:206-13; PMID:20305381; http://dx.doi.org/10.4161/epi.5.3.11447
5. Zilberman D. The human promoter methylome. Nat Genet 2007; 39:442-3; PMID:17392803; http://dx.doi.org/10.1038/ng0407-442
6. Hitchins MP, Wong JJL, Suthers G, Suter CM, Martin DIK, Hawkins NJ, Ward RL. Inheritance of a cancer-associated MLH1 germ-line epimutation. N Engl J Med 2007; 356:697-705; PMID:17301300; http://dx.doi.org/10.1056/NEJMoa064522
7. Chan TL, Yuen ST, Kong CK, Chan YW, Chan ASY, Ng WF, Tsui WY, Lo MWS, Tam WY, Li VSW, et al. Heritable germline epimutation of MSH2 in a family with hereditary nonpolyposis colorectal cancer. Nat Genet 2006; 38:1178-83; PMID:16951683; http://dx.doi.org/10.1038/ng1866

8. Crucianelli F, Tricarico R, Turchetti D, Gorelli G, Gensini F, Sestini R, Giunti L, Pedroni M, Ponz de Leon M, Civitelli S, et al. MLH1 constitutional and somatic methylation in patients with MLH1 negative tumors fulfilling the revised Bethesda criteria. Epigenetics 2014; 9:1431-8; PMID:25437057; http://dx.doi.org/10.4161/15592294.2014.970080

9. Galetzka D, Hansmann T, El Hajj N, Weis E, Irmscher B, Ludwig M, Schneider-Rätzke B, Kohlschmidt N, Beyer V, Bartsch O, et al. Monozygotic twins discordant for constitutive BRCA1 promoter methylation, childhood cancer and secondary cancer. Epigenetics 2012; 7:47-54; PMID:22207351; http://dx.doi.org/10.4161/epi.7.1.18814

10. Hansmann T, Pliushch G, Leubner M, Kroll P, Endt D, Gehrig A, Preisler-Adams S, Wieacker P, Haaf T. Constitutive promoter methylation of BRCA1 and RAD51C in patients with familial ovarian cancer and early-onset sporadic breast cancer. Hum Mol Genet 2012; 21:4669-79; PMID:22843497; http://dx.doi.org/10.1093/hmg/dds308

11. Tapia T, Smalley S V, Kohen P, Muñoz A, Solis LM, Corvalan A, Faundez P, Devoto L, Camus M, Alvarez M, et al. Promoter hypermethylation of BRCA1 correlates with absence of expression in hereditary breast cancer tumors. Epigenetics 2008; 3:157-63; PMID:18567944; http://dx.doi.org/10.4161/epi.3.3.6387

12. Turner N, Tutt A, Ashworth A. Hallmarks of "BRCAness" in sporadic cancers. Nat Rev Cancer 2004; 4:814-9; PMID:15510162; http://dx.doi.org/10.1038/nrc1457

13. Stefansson OA, Villanueva A, Vidal A, Martí L, Esteller M. BRCA1 epigenetic inactivation predicts sensitivity to platinum-based chemotherapy in breast and ovarian cancer. Epigenetics 2012; 7:1225-9; PMID:23069641; http://dx.doi.org/10.4161/epi.22561

14. Vogel W, Surowy H. Reduced DNA repair in BRCA1 mutation carriers undetectable before onset of breast cancer? Br J Cancer 2007; 97:1184-6; author reply 1187; PMID:17848944; http://dx.doi.org/10.1038/sj.bjc.6603977

15. Salem AF, Howell A, Sartini M, Sotgia F, Lisanti MP. Downregulation of stromal BRCA1 drives breast cancer tumor growth via upregulation of HIF-1α, autophagy and ketone body production. Cell Cycle 2012; 11:4167-73; PMID:23047605; http://dx.doi.org/10.4161/cc.22316

16. Milner R, Wombwell H, Eckersley S, Barnes D, Warwicker J, Van Dorp E, Rowlinson R, Dearden S, Hughes G, Harbron C, et al. Validation of the BRCA1 antibody MS110 and the utility of BRCA1 as a patient selection biomarker in immunohistochemical analysis of breast and ovarian tumors. Virchows Arch 2013; 462:269-79; PMID:23354597; http://dx.doi.org/10.1007/s00428-012-1368-y

17. Rinn JL, Bondre C, Gladstone HB, Brown PO, Chang HY. Anatomic demarcation by positional variation in fibroblast gene expression programs. PLoS Genet 2006; 2:e119; PMID:16895450; http://dx.doi.org/10.1371/journal.pgen.0020119

18. Vuillaume ML, Uhrhammer N, Vidal V, Vidal VS, Chabaud V, Jesson B, Kwiatkowski F, Bignon Y-J. Use of gene expression profiles of peripheral blood lymphocytes to distinguish BRCA1 mutation carriers in high risk breast cancer families. Cancer Inform 2009; 7:41-56; PMID:19352458

19. Bhowmick NA, Neilson EG, Moses HL. Stromal fibroblasts in cancer initiation and progression. Nature 2004; 432:332-7; PMID:15549095; http://dx.doi.org/10.1038/nature03096

20. Zeisberg EM, Potenta S, Xie L, Zeisberg M, Kalluri R. Discovery of endothelial to mesenchymal transition as a source for carcinoma-associated fibroblasts. Cancer Res 2007; 67:10123-8; PMID:17974953; http://dx.doi.org/10.1158/0008-5472.CAN-07-3127

21. Kalluri R, Zeisberg M. Fibroblasts in cancer. Nat Rev Cancer 2006; 6:392-401; PMID:16572188; http://dx.doi.org/10.1038/nrc1877

22. Iwano M, Plieth D, Danoff TM, Xue C, Okada H, Neilson EG. Evidence that fibroblasts derive from epithelium during tissue fibrosis. J Clin Invest 2002; 110:341-50; PMID:12163453; http://dx.doi.org/10.1172/JCI0215518

23. Kojima Y, Acar A, Eaton EN, Mellody KT, Scheel C, Ben-Porath I, Onder TT, Wang ZC, Richardson AL, Weinberg RA, et al. Autocrine TGF-β and stromal cell-derived factor-1 (SDF-1) signaling drives the evolution of tumor-promoting mammary stromal myofibroblasts. Proc Natl Acad Sci U S A 2010; 107:20009-14; PMID:21041659; http://dx.doi.org/10.1073/pnas.1013805107

24. Erez N, Truitt M, Olson P, Arron ST, Hanahan D. Cancer-Associated Fibroblasts Are Activated in Incipient Neoplasia to Orchestrate Tumor-Promoting Inflammation in an NF-kappaB-Dependent Manner. Cancer Cell 2010; 17:135-47; PMID:20138012; http://dx.doi.org/10.1016/j.ccr.2009.12.041

25. Trimboli AJ, Cantemir-Stone CZ, Li F, Wallace JA, Merchant A, Creasap N, Thompson JC, Caserta E, Wang H, Chong JL, et al. Pten in stromal fibroblasts suppresses mammary epithelial tumors. Nature 2009; 461:1084-91; PMID:19847259; http://dx.doi.org/10.1038/nature08486

26. Pickard A, Cichon AC, Barry A, Kieran D, Patel D, Hamilton P, Salto-Tellez M, James J, McCance DJ. Inactivation of Rb in stromal fibroblasts promotes epithelial cell invasion. EMBO J 2012; 31:3092-103; PMID:22643222; http://dx.doi.org/10.1038/emboj.2012.153

27. Lee KW, Yeo SY, Sung CO, Kim SH. Twist1 is a key regulator of cancer-associated fibroblasts. Cancer Res 2015; 75:73-85; PMID:25368021; http://dx.doi.org/10.1158/0008-5472.CAN-14-0350

28. Guido C, Whitaker-Menezes D, Capparelli C, Balliet R, Lin Z, Pestell RG, Howell A, Aquila S, Andò S, Martinez-Outschoorn U, et al. Metabolic reprogramming of cancer-associated fibroblasts by TGF-β drives tumor growth: connecting TGF-β signaling with "Warburg-like" cancer metabolism and L-lactate production. Cell Cycle 2012; 11:3019-35; PMID:22874531; http://dx.doi.org/10.4161/cc.21384

29. Yeung TL, Leung CS, Wong KK, Samimi G, Thompson MS, Liu J, Zaid TM, Ghosh S, Birrer MJ, Mok SC. TGF-β modulates ovarian cancer invasion by upregulating CAF-derived versican in the tumor microenvironment. Cancer Res 2013; 73:5016-28; PMID:23824740; http://dx.doi.org/10.1158/0008-5472.CAN-13-0023

30. Sanchez-Alvarez R, Martinez-Outschoorn UE, Lin Z, Lamb R, Hulit J, Howell A, Sotgia F, Rubin E, Lisanti MP. Ethanol exposure induces the cancer-associated fibroblast phenotype and lethal tumor metabolism: implications for breast cancer prevention. Cell Cycle 2013; 12:289-301; PMID:23257780; http://dx.doi.org/10.4161/cc.23109

31. Valin A, Barnay-Verdier S, Robert T, Ripoche H, Brellier F, Chevallier-Lagente O, Avril M-F, Magnaldo T. PTCH1 +/− dermal fibroblasts isolated from healthy skin of Gorlin syndrome patients exhibit features of carcinoma associated fibroblasts. PLoS One 2009; 4:e4818; PMID:19287498; http://dx.doi.org/10.1371/journal.pone.0004818

32. De Luca P, Moiola CP, Zalazar F, Gardner K, Vazquez ES, De Siervi A. BRCA1 and p53 regulate critical prostate cancer pathways. Prostate Cancer Prostatic Dis 2013; 16:233-8; PMID:23670255; http://dx.doi.org/10.1038/pcan.2013.12

33. Durning P, Schor SL, Sellwood RA. Fibroblasts from patients with breast cancer show abnormal migratory behaviour in vitro. Lancet 1984; 2:890-2; PMID:6148619; http://dx.doi.org/10.1016/S0140-6736(84)90653-6

34. Haggie JA, Sellwood RA, Howell A, Birch JM, Schor SL. Fibroblasts from relatives of patients with hereditary breast cancer show fetal-like behaviour in vitro. Lancet 1987; 1:1455-7; PMID:2885452; http://dx.doi.org/10.1016/S0140-6736(87)92206-9

35. Furuta S, Jiang X, Gu B, Cheng E, Chen PL, Lee WH. Depletion of BRCA1 impairs differentiation but enhances proliferation of mammary epithelial cells. Proc Natl Acad Sci U S A 2005; 102:9176-81; PMID:15967981; http://dx.doi.org/10.1073/pnas.0503793102

36. Thompson ME, Jensen RA, Obermiller PS, Page DL, Holt JT. Decreased expression of BRCA1 accelerates growth and is often present during sporadic breast cancer progression. Nat Genet 1995; 9:444-50; PMID:7795653; http://dx.doi.org/10.1038/ng0495-444

37. Mar PK, Roy P, Yin HL, Cavanagh HD, Jester JV. Stress fiber formation is required for matrix reorganization in a corneal myofibroblast cell line. Exp Eye Res 2001; 72:455-66; PMID:11273673; http://dx.doi.org/10.1006/exer.2000.0967

38. Antecol MH, Darveau A, Sonenberg N, Mukherjee BB. Altered biochemical properties of actin in normal skin fibroblasts from individuals predisposed to dominantly inherited cancers. Cancer Res 1986; 46:1867-73; PMID:3948169

39. Bonuccelli G, Tsirigos A, Whitaker-Menezes D, Pavlides S, Pestell RG, Chiavarina B, Frank PG, Flomenberg N, Howell A, Martinez-Outschoorn UE, et al. Ketones and lactate "fuel" tumor growth and metastasis: Evidence that epithelial cancer cells use oxidative mitochondrial

metabolism. Cell Cycle 2010; 9:3506-14; PMID:20818174; http://dx.doi.org/10.4161/cc.9.17.12731

40. Martinez-Outschoorn UE, Lin Z, Whitaker-Menezes D, Howell A, Lisanti MP, Sotgia F. Ketone bodies and two-compartment tumor metabolism: stromal ketone production fuels mitochondrial biogenesis in epithelial cancer cells. Cell Cycle 2012; 11:3956-63; PMID:23082721; http://dx.doi.org/10.4161/cc.22136

41. Pavlides S, Whitaker-Menezes D, Castello-Cros R, Flomenberg N, Witkiewicz AK, Frank PG, Casimiro MC, Wang C, Fortina P, Addya S, et al. The reverse Warburg effect: aerobic glycolysis in cancer associated fibroblasts and the tumor stroma. Cell Cycle 2009; 8:3984-4001; PMID:19923890; http://dx.doi.org/10.4161/cc.8.23.10238

42. Martinez-Outschoorn UE, Balliet RM, Rivadeneira DB, Chiavarina B, Pavlides S, Wang C, Whitaker-Menezes D, Daumer KM, Lin Z, Witkiewicz AK, et al. Oxidative stress in cancer associated fibroblasts drives tumor-stroma co-evolution: A new paradigm for understanding tumor metabolism, the field effect and genomic instability in cancer cells. Cell Cycle 2010; 9:3256-76; PMID:20814239

43. Hyo JK, Hee JK, Rih J-KK, Mattson TL, Kyu WK, Cho C-HH, Isaacs JS, Bae I, Kang HJ, Kim HJ, et al. BRCA1 plays a role in the hypoxic response by regulating HIF-1alpha stability and by modulating vascular endothelial growth factor expression. J Biol Chem 2006; 281:13047-56; PMID:16543242; http://dx.doi.org/10.1074/jbc.M513033200

44. Martinez-Outschoorn UE, Trimmer C, Lin Z, Whitaker-Menezes D, Chiavarina B, Zhou J, Wang C, Pavlides S, Martinez-Cantarin MP, Capozza F, et al. Autophagy in cancer associated fibroblasts promotes tumor cell survival: Role of hypoxia, HIF1 induction and NFκB activation in the tumor stromal microenvironment. Cell Cycle 2010; 9:3515-33; PMID:20855962; http://dx.doi.org/10.4161/cc.9.17.12928

45. Xu LN, Xu BN, Cai J, Yang JB, Lin N. Tumor-associated fibroblast-conditioned medium promotes tumor cell proliferation and angiogenesis. Genet Mol Res 2013; 12:5863-71; PMID:24301956; http://dx.doi.org/10.4238/2013.November.22.14

46. Subramaniam KS, Tham ST, Mohamed Z, Woo YL, Mat Adenan NA, Chung I. Cancer-associated fibroblasts promote proliferation of endometrial cancer cells. PLoS One 2013; 8:e68923; PMID:23922669; http://dx.doi.org/10.1371/journal.pone.0068923

47. Gong X, Yi J, Carmon KS, Crumbley CA, Xiong W, Thomas A, Fan X, Guo S, An Z, Chang JT, et al. Aberrant RSPO3-LGR4 signaling in Keap1-deficient lung adenocarcinomas promotes tumor aggressiveness. Oncogene 2015; 34:4692-701; PMID:25531322; http://dx.doi.org/10.1038/onc.2014.417

48. Carmon KS, Gong X, Yi J, Thomas A, Liu Q. RSPO-LGR4 functions via IQGAP1 to potentiate Wnt signaling. Proc Natl Acad Sci U S A 2014; 111:E1221-9; PMID:24639526; http://dx.doi.org/10.1073/pnas.1323106111

49. Calon A, Tauriello DVF, Batlle E. TGF-β in CAF-mediated tumor growth and metastasis. Semin Cancer Biol 2014; 25:15-22; PMID:24412104; http://dx.doi.org/10.1016/j.semcancer.2013.12.008

50. Martinez-Outschoorn UE, Balliet R, Lin Z, Whitaker-Menezes D, Birbe RC, Bombonati A, Pavlides S, Lamb R, Sneddon S, Howell A, et al. BRCA1 mutations drive oxidative stress and glycolysis in the tumor microenvironment: implications for breast cancer prevention with antioxidant therapies. Cell Cycle 2012; 11:4402-13; PMID:23172369; http://dx.doi.org/10.4161/cc.22776

51. Huang DW, Sherman BT, Lempicki RA. Systematic and integrative analysis of large gene lists using DAVID bioinformatics resources. Nat Protoc 2009; 4:44-57; PMID:19131956; http://dx.doi.org/10.1038/nprot.2008.211

52. Untergasser A, Cutcutache I, Koressaar T, Ye J, Faircloth BC, Remm M, Rozen SG. Primer3–new capabilities and interfaces. Nucleic Acids Res 2012; 40:e115; PMID:22730293; http://dx.doi.org/10.1093/nar/gks596

53. Bräutigam C, Raggioli A, Winter J. The Wnt/β-catenin pathway regulates the expression of the miR-302 cluster in mouse ESCs and P19 cells. PLoS One 2013; 8:e75315; http://dx.doi.org/10.1371/journal.pone.0075315